

Lateral Earth Pressure and Stability of Quay Walls During Earth-Quakes

By HARUO MATUO¹ and SUKEO ŌHARA²

Abstract

After the great Kantō earthquake of 1923 in Japan, it became necessary to know the earth pressure which acts on the wall during earthquakes, in the reconstruction work of quay walls of Yokohama Harbour. Prof. Mononobe and Dr. Okabe proposed an idea to compute the pressure. They assumed that the resultant force due to max seismic acceleration and acceleration of gravity, acts statically, and adapting Coulomb's theory, computed the seismic earth pressure.

According to this computation, intensity of the earth pressure, to be added to static pressure, increases linearly as the depth.

But the experiment shows that this pressure is larger near the surface than near the bottom, contrary to the result above mentioned.

The authors here propose a new formula for it, and comparing with the results of their experiments, conclude that they bear good resemblance to each other.

Earth Pressure During Vibration

a) Theoretical computation

Seismic earth pressure against a vertical wall was theoretically computed by assuming the earth as a uniform elastic medium of two dimensions. X axis is taken horizontally along the boundary surface at the base of a solid wall, and y axis vertically upward along the back surface of the wall (Fig. 1 a).

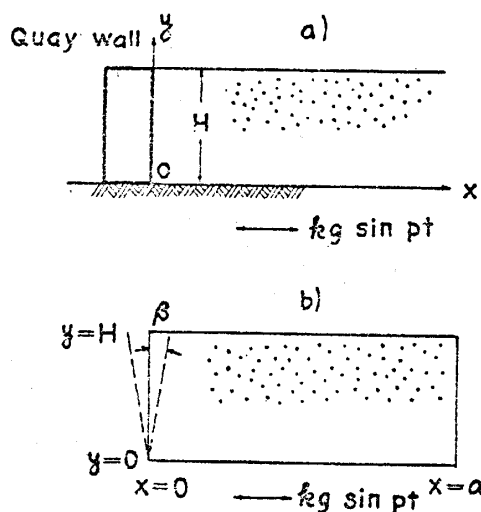


Fig. 1 a) Fixed Wall
b) Movable Wall

$$\left. \begin{aligned} (\lambda + \mu) \frac{\partial \Delta}{\partial x} + \mu \nabla^2 u + \rho k g \sin pt &= \rho \frac{\partial^2 u}{\partial t^2} \\ (\lambda + \mu) \frac{\partial \Delta}{\partial y} + \mu \nabla^2 v &= \rho \frac{\partial^2 v}{\partial t^2} \end{aligned} \right\} \quad (1)$$

Boundary conditions

$$\begin{aligned} \text{i) } & (u)_{x=0} = (u)_{y=0} = 0 \\ \text{ii) } & (v)_{x=0} = (v)_{y=0} = 0 \\ \text{iii) } & \left(\lambda \Delta + 2\mu \frac{\partial v}{\partial y} \right)_{y=H} = 0 \\ \text{iv) } & \mu \left(\frac{\partial u}{\partial y} + \frac{\partial v}{\partial x} \right)_{y=H} = 0 \end{aligned}$$

where u, v = Components of displacements for x and y direction.

λ, μ = Lamè's elastic constants.

k = Seismic coefficients.

ρ = Density

General solution of the equation is not easily obtained, but the solution for the equation (1) has intermediate values between the two extreme cases of (A) and (B).

(A) When the displacement of y direction is perfectly restricted,

(B) When no resistance exists against the displacement of y direction.

For both these cases the following equation holds good approximation.

$$C_1^2 \frac{\partial^2 u}{\partial x^2} + C_2^2 \frac{\partial^2 u}{\partial y^2} + k g \sin pt = \frac{\partial^2 u}{\partial t^2} \quad (2)$$

Boundary conditions,

$$\begin{aligned} \text{i) } & (u)_{x=0} = (u)_{y=0} = 0 \\ \text{ii) } & \left(\frac{\partial u}{\partial y} \right)_{y=H} = 0 \end{aligned}$$

For the equation (2), the solution is easily obtained as follows

$$\begin{aligned} u = \frac{kg}{p^2} \left\{ \frac{2}{H} \sum_m \frac{-\frac{2H}{2(m+1)\pi} \left(\frac{p}{C_2} \right)^2}{\left(\frac{(2m+1)\pi}{2H} \right)^2 - \left(\frac{p}{C_2} \right)^2} e^{-\frac{C_2}{C_1} \sqrt{\left(\frac{(2m+1)\pi}{2H} \right)^2 - \left(\frac{p}{C_2} \right)^2} \cdot x} \cdot \sin \frac{(2m+1)\pi}{2H} y \right. \\ \left. + \tan \frac{p}{C_2} H \cdot \sin \frac{p}{C_2} y + \cos \frac{p}{C_2} y \right\} \sin pt \quad (3) \end{aligned}$$

and from this we have as the max half amplitude σ_x of vibrating pressure at the wall as

$$(\sigma_x)_{x=0} = -\rho \sum_m \frac{4kg \sin pt}{\pi(2m+1) \sqrt{\frac{C_2^2}{C_1^2} \left(\frac{(2m+1)\pi}{2} \right)^2 - \left(\frac{pH}{C_1} \right)^2}} \cdot \sin \frac{(2m+1)\pi}{2} \eta \quad (4)$$

in which $\eta = y/H$

Here for the case (A) $c_1^2 = (\lambda + 2\mu)/\rho$, $c_2^2 = \mu/\rho$

and for the case (B) $c_1^2 = E/\rho(1 - \nu^2)$, $c_2^2 = \mu/\rho$

$E = \text{Young's Modulus}$; $\nu = \text{Poisson's ratio}$.

The value of σ_x for (A) is larger than for (B); The difference between the two being about 10% when $\nu = 0.3$.

For safety's sake we may take the equation for the case (A) as the approximate equation of (1), and the solution of which as the approximate one for the design of aseismic quay walls.

Furthermore it was found by another research of ours that the values of c_1^2 and c_2^2 changes if proportion to the depth from the earth surface. Therefore equation (2) is changed to the equation having variable coefficients as follows,

$$\frac{\partial^2 U}{\partial t^2} = \frac{C_1^2}{a^2} (1 - \alpha_1 \eta) \frac{\partial^2 U}{\partial \xi^2} + \frac{\partial}{\partial \eta} \left[\frac{C_2^2}{H} (1 - \alpha_2 \eta) \frac{\partial U}{\partial \eta} \right] + \frac{kg}{H} \sin pt \quad (5)$$

Boundary conditions

$$\text{i) } (U)_{\xi=0} = (U)_{\eta=0} = (U)_{\xi=1} = 0$$

$$\text{ii) } \left(\frac{\partial U}{\partial \eta} \right)_{\eta=1} = 0$$

where

$$\xi = x/a, \quad \eta = y/H, \quad U = u/H$$

Ritz's approximate solution was applied and we have the approximate solution as follows.

$$U = \sum_{mn} A_{mn} \sin \frac{(2m+1)\pi}{2} \eta \cdot \sin (2m+1)\pi \xi, \sin pt \quad (6)$$

and from this σ_x as follows;

$$(\sigma_x)_{x=0} = -C_1^2 (1 - \alpha_1 \eta) \rho \frac{H}{a} \sum_{mn} (2m+1)\pi A_{mn} \sin \frac{(2m+1)\pi}{2} \eta \cdot \sin pt \quad (7)$$

When there is surcharge of intensity q on the earth surface, the equation (5) is to be solved by the following boundary conditions.

$$\text{i) } (U)_{\eta=0} = 0$$

$$\text{ii) } \frac{\rho C_2^2 (1 - \alpha_2)}{H} \left(\frac{\partial U}{\partial \eta} \right)_{\eta=1} = \frac{kg}{H} \sin pt + p^2 \frac{q}{g} (U)_{\eta=1}$$

$$\text{iii) } (U)_{\xi=0} = (U)_{\xi=1} = 0$$

In this case as Ritz's solution cannot be applied, and therefore different method was applied and σ_x was obtained.

b) Experiments

In the experiments which were carried out in our laboratory, the intensity of the horizontal earth pressure was measured at the end wall of a box on a shaking table.

Two kinds of end walls were used, "fixed" vertical wall and "movable" one, both perpendicular to the direction of vibration.

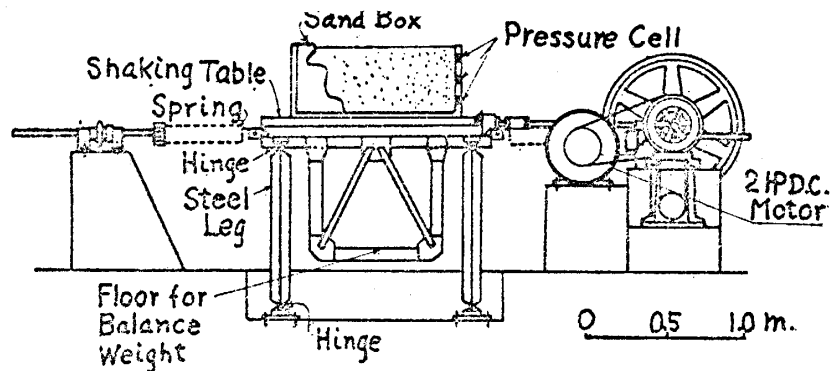


Fig. 2 Shaking table.

The shaking table (Fig. 2) was supported by 4 vertical rigid steel strips with free hinged ends, and laterally supported by two pairs of spiral springs, and was driven by a crank shaft connected to an eccentric disk. Two kinds of boxes were used; the one a steel box having the dimensions 40 (height) \times 90 (width) \times 100 (length) cm, and the other a wooden box with a glass side 40 \times 50 \times 100 cm.

Earth pressure was measured by pressure cells with a disk of 3.4 cm diameter connected to a steel cross beam. The deformation of the beam was measured by electric strain meters attached to it (Fig. 3). The deformation of the beam at the center was 0.5×10^{-4} mm/g/cm².

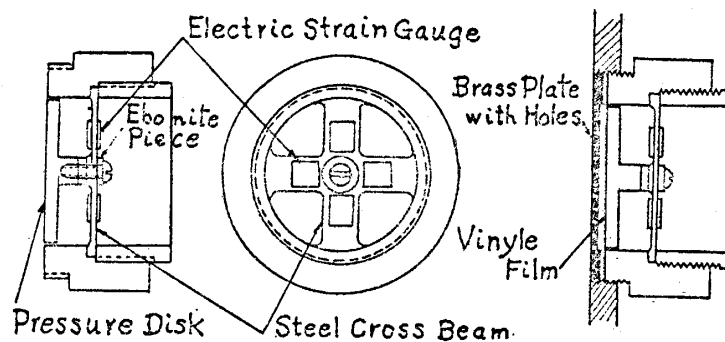


Fig. 3 Pressure cells

- a) for earth and pore pressure,
- b) for pore pressure only.

In the first experiment dry sand was carefully filled in the box and pressure changes were measured at 3 different heights along the center line of the end wall.

The results in case of a "fixed" wall are shown in Fig. 4 and 5a. The sand had mean diameter of 1.0 mm and uniformity coefficient of 6.1; the period of vibration

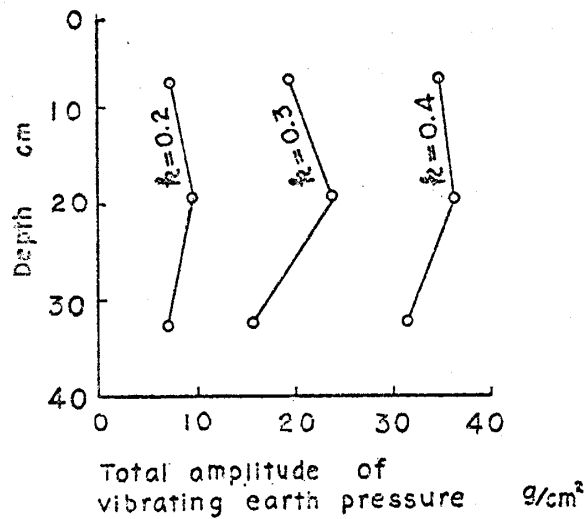


Fig. 4 Amplitude of vibrating pressure for rigid wall at 3 different heights (observed mean values).

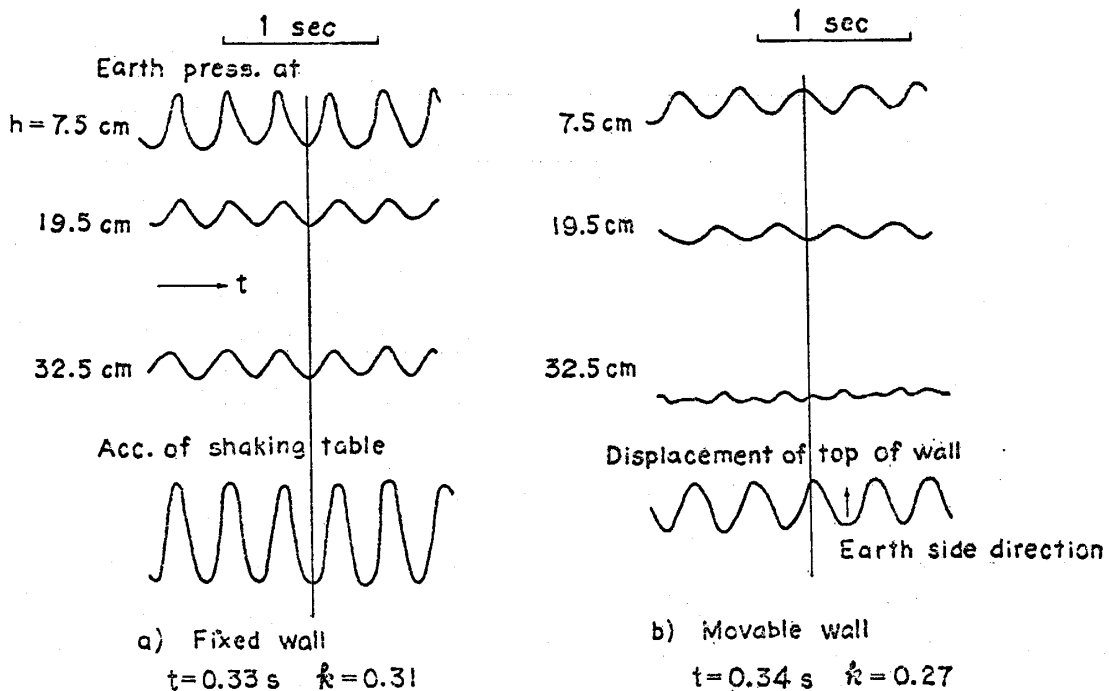


Fig. 5 Record of pressure change at 3 different heights as compared with the acc. of the shaking table or the displacement of the top of the wall.

- a) Fixed wall-for 3 heights the phase is the same.
- b) Movable wall-here the phase of 7.5 cm is different from 19.5 cm.

being $T=0.3$ sec. After the dry sand was filled uniformly in loose condition, the vibration was given in such a way that the amplitude gradually increases for about 7 seconds, and then remains constant for about 10 seconds, and then gradually decreases to a standstill in about 7 seconds. Fig. 4 shows the double amplitude of pressure change at the beginning of vibration, and Fig. 5 a is the record of pressure during vibration.

As may be seen from Fig. 4, the amplitude of pressure change is large at middle height, the phase of pressure change being the same throughout the whole depth. Fig. 2 a shows that there was no phase difference between the pressures of 3 different heights.

Fig. 5 b is the record of pressure in case of a "movable" wall. In this case a wall with a hinge at the lower end was vertically supported by a rod resting on an elastic spring plate. From this experiment we could see that

- 1) Max amplitude of pressure decreases as the displacement increases, so long as the displacement is below a certain value.
- 2) When the amount of displacement exceeds the value, phase difference appears between the pressures at different heights, as shown in Fig. 5 b.

Two series of field experiments are now going on. Earth pressure acting on a concrete wall (Height 1.5 m, width 0.9 m, length 2.0 m) is measured at 5 different heights (Fig. 6). Vibration is given 1) externally by an oscillator of 1 HP set at the

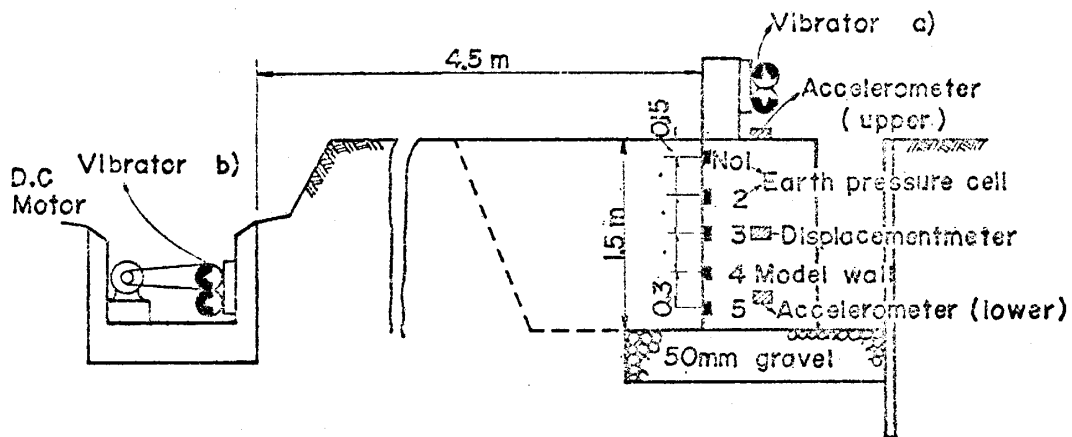


Fig. 6 Fields test arrangements.

distance of 4.5 m from the wall surface, and 2) internally by the oscillator of 200 Watts set at the top of the wall. The acceleration and displacement are measured at 3 different heights on the wall. Some of the results are shown in Fig. 7 and Fig. 8. By comparing the results of externally and internally excited vibrations, actual seismic earth pressure may be computed. The results of which will be made public at the next chance.

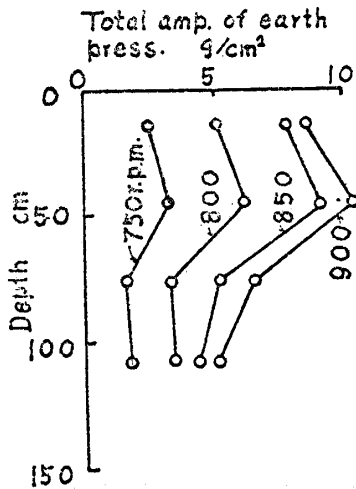


Fig. 7 Field test results, when vibration was given to the ground at 4.5 m distant from the wall.

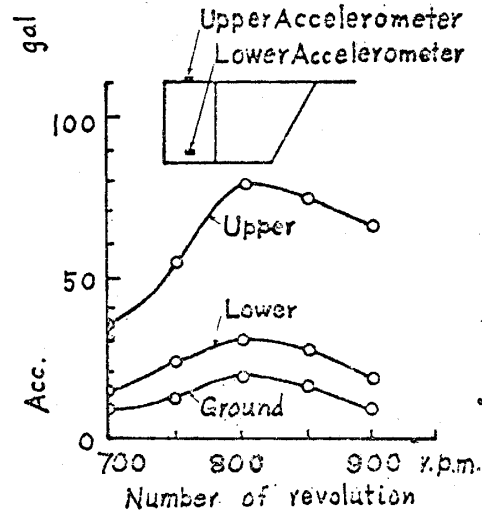


Fig. 8 Field test results, when vibration was given to the ground at 4.5 m distant from the wall.

c) Comparison of the theoretical and experimental results.

Elastic constants of the sand were determined by another experiments; and from these constants c_1^2 , c_2^2 , α_1 and α_2 were determined. Applying these values for the solution of equation (5), the seismic earth pressure for a "fixed" wall was computed and the results are shown in Fig. 9. The distribution of pressure is akin to that of observed values (Fig. 4).

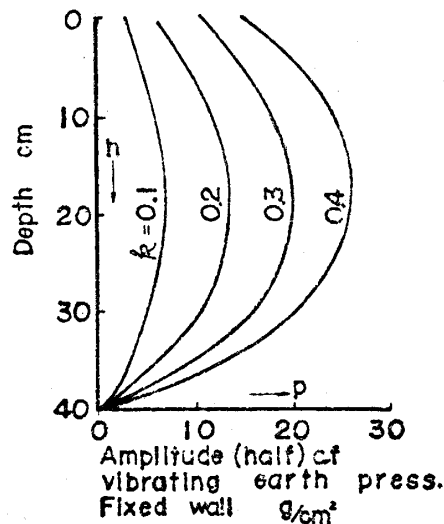


Fig. 9 Computed amplitude of vibrating earth pressure (half amp.); fixed wall.

In Fig. 10 total amplitudes of pressure are plotted against k for 3 different heights. In this figure mean values can be roughly represented by the chain lines, excluding the values larger than $k=0.3$. At larger acceleration than $k=0.3$, relative movement of sand particles occurs, which is not assumed in our computation.

In the figure the full lines, which indicate the computed values corresponding to the observed ones, are lower than the chain lines. But the inclinations of the two lines are

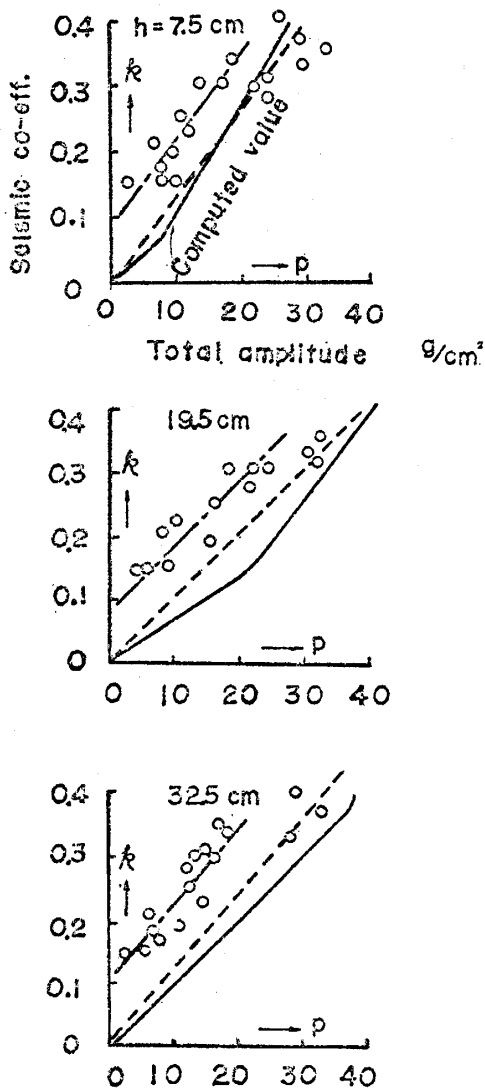


Fig. 10 Observed and computed value at 3 different heights. Full line is computed values, and the chain line is the mean observed value.

nearly the same. This may be attributed to the effect of side walls of the box and the elasticity of the pressure cells.

Here, "total" amplitude does not always mean double amplitude; at small depth, static pressure becomes less than absolute value of the vibrating minus pressure when k exceeds a certain value, but as there is no tension between the earth mass and the wall, the "total" amplitude at such a depth is smaller than the double amplitude and equal to the sum of the static pressure and the half amplitude. As plus and minus pressures can not be distinguished in the observation, the total amplitudes of pressures are plotted and compared with the computed value.

An approximate solution for the movable wall was obtained by adding the solution of the following formula (8) to the solution of (5) of fixed wall (Fig. 3 b). This is the solution when the wall itself rotates by the angular amplitude β .

$$\frac{\partial^2 U}{\partial t^2} = \frac{C_1^2}{a^2} (1 - \alpha_1 \eta) \frac{\partial^2 U}{\partial \xi^2} + \frac{\partial}{\partial \eta} \left[\frac{C_2^2}{H^2} (1 - \alpha_2 \eta) \frac{\partial U}{\partial \eta} \right] \quad (8)$$

Boundary conditions

- i) $(U)_{\xi=0} = \beta\eta \sin pt$
- ii) $(U)_{\xi=1} = (U)_{\eta=0} = 0$
- iii) $\left(\frac{\partial U}{\partial \eta}\right)_{\eta=1} = 0$

To solve (8), put

$$U = \sum_{mn} A_{mn} \sin \frac{(2m+1)\pi}{2} \eta \cdot \frac{\sinh \sqrt{\lambda_n}(1-\xi)}{\sinh \sqrt{\lambda_n}} \sin pt \tag{9}$$

where

$$U = \frac{u}{H}, \quad \xi = \frac{x}{a}, \quad \eta = \frac{y}{H}$$

Applying Ritz's approximate solution, λ_n was determined, and then approximate values of A_{mn} . $(\sigma_x)_{x=0}$ should be determined from (9), but when $x=0$, σ_x does not converge,

$$(\sigma_x)_{x=\varepsilon} = C_1^2(1-\alpha_1\eta)\rho \sum_{mn} \frac{H}{a} \sqrt{\lambda_n} A_{mn} \sin \frac{(2m+1)}{2} \eta \times \frac{\cosh \sqrt{\lambda_n}(1-\varepsilon)}{\sinh \sqrt{\lambda_n}} \tag{10}$$

was taken as the approximate value of $(\sigma_x)_{x=0}$, where ε is infinite small value.

The solution of (8) has sign opposite to the solution of (5) and the resulting distribution of pressure becomes as shown with full line in Fig. 11. From this, the phenomena that the pressure of different heights has opposite signs (Fig. 1 and 5 b) can be explained.

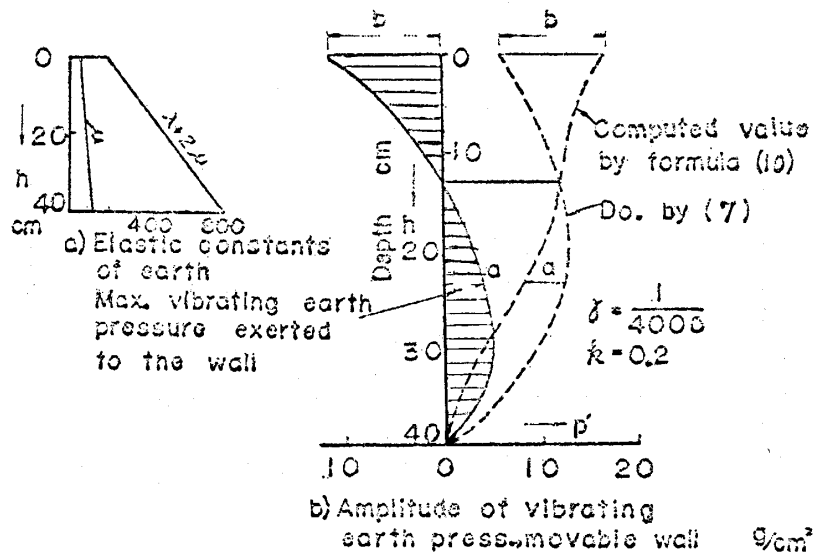


Fig. 11 Computed pressure to be exerted to a movable wall.

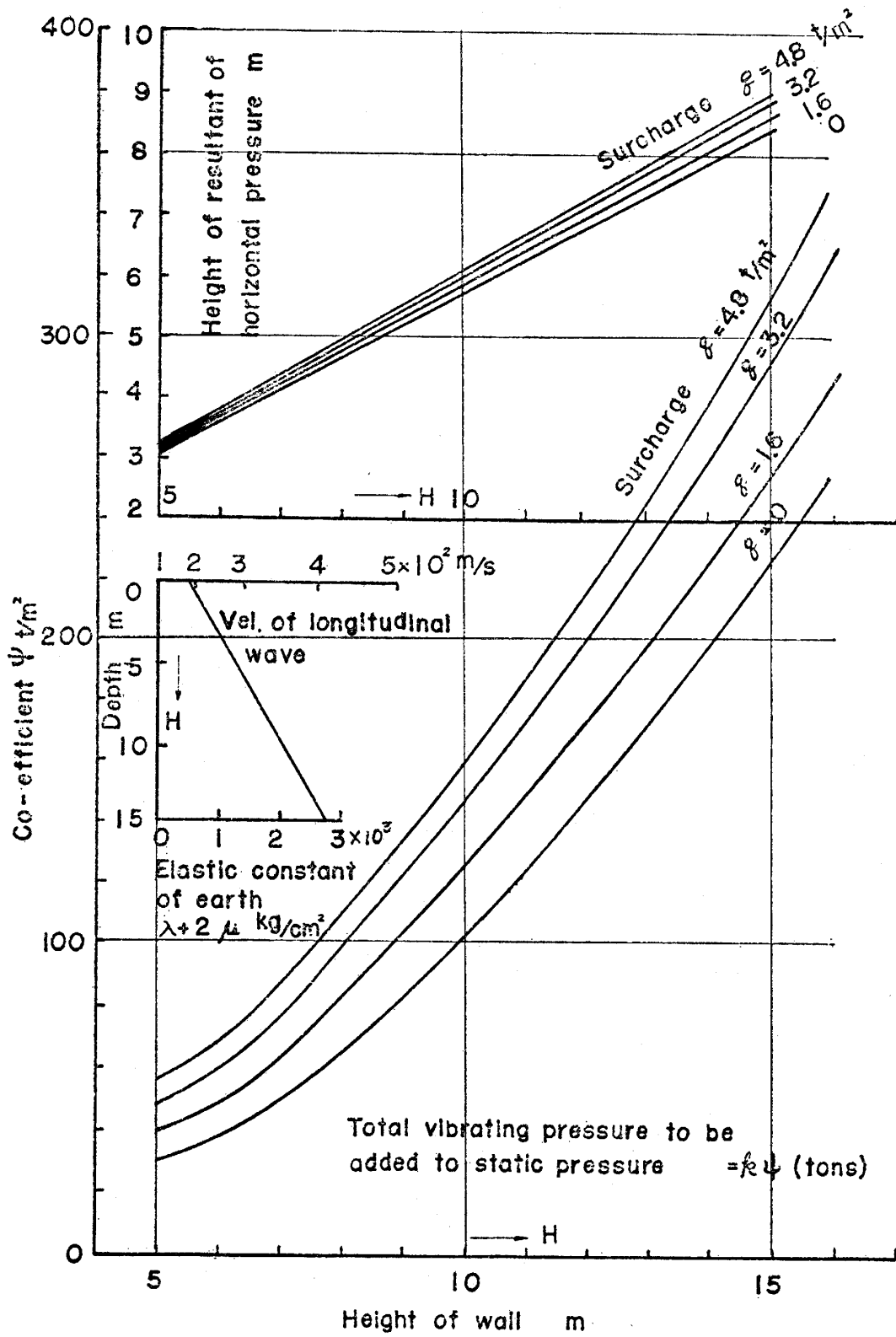


Fig. 12 Computed earth pressures which should be added to static pressures and point of application of the resultant force.

Earth Pressure Diagrams

Max earth pressure against quay walls during earthquakes is calculated according to formula (7), assuming the wall to be "fixed", and it is shown in Fig. 12. In the calculation of stability, total earth pressure is obtained by adding above pressure to ordinary static earth pressure. Here ρ is taken as 1.6 gr/cm^3 , and the elastic constants of the back filling is taken as shown in the accompanying figure in Fig. 12. Total pressure $P = k\psi$, where k is the seismic coefficient, and ψ is to be read on the diagram for various surcharge q . The height of point of application of the resultant pressure can be read on the upper diagram. Here the resonance of the earthquake vibration and earth pressure is disregarded, assuming the period of earthquake vibration is pretty larger than that of earth pressure.

To make the calculation simple, the width of the whole back-filling was assumed 10 times as large as the quay wall height, because the seismic pressure thus calculated is approximately the same with infinitely long back-filling. When seismic earth pressure and pore pressure are at their max the water pressure to the wall from the sea decreases in accordance to the Westergaard's formula, and it is under this condition that the stability of the wall is calculated.

Conclusions

According to theoretical study, the distribution of seismic earth pressure is computed as shown in Fig. 9, and total pressure and point of application acting on a vertical wall were calculated as shown in Fig. 12. For this calculation it was assumed that the wall is "fixed", not allowing any relative displacement against the ground, and that there is no resonance between the ground motion and the earth pressure. These conditions may not be satisfied always, and for the case further research is expected in future. The results of experiments may be said nearly to coincide with the theoretical computation for "fixed" wall.

Theoretical computation for "movable" wall could explain the experimental fact that the seismic pressures of plus and minus values coexist at different heights of the wall. The phenomenon of liquefaction of saturated sand due to vibration was observed, but it was concluded that, when there is rip-rup between the wall and the sand-filling, the pressure of liquefied earth does not act on the wall.

Bibliography

- Mononobe, N. "Design of a seismic Gravity Wall." Report of Kantō Earthquake Damages of 1923. J. S. C. E. Vol. 3, 1925
- Okabe, S. "General Theory of Earth Pressure and Seismic Stability of Retaining Wall and Dam." (in English) Jour. J. S. C. E. Vol. 12, No. 1, 1924.
- Matuo, H. "Experimental Study on the Distribution of Lateral Earth Pressure in Earthquakes."

Jour. J. S. C. E. Vol. 27, No. 2, 1941

Matuo, H. & Ohara, S. "Seismic Earth Pressure due to Saturated Soils." Jour. J. S. C. E. Vol. 40, No. 6, 1955

Matuo, H. & Ohara, S. "Seismic Earth Pressure against Quay Walls." Technical Report of Kyushu Univ. Vol. 29, No. 2, 1956; Vol. 30, No. 1, 1957; Vol. 31, No. 2, 1958

Ohara, S. "Determination of Elastic Constants of Sand." Transactions, J. S. C. E. No. 38, 1956

Niwa, S. "Study on Vibrating Earth Pressure." Monthly Reports of Transportation Technical Research Institute, Vol. 8, No. 3, 1958

Nomenclature

a = Length of the earth filling

$c_1^2 = (\lambda + 2\mu)/\rho$ or $E/\rho(1 - \nu^2)$

$c_2^2 = \mu/\rho$

E = Young's modulus

k = Seismic coefficient viz. acceleration of earthquake divided by acceleration of gravity

H = Height of the wall

$p = 2\pi/T$

T = Period of vibration

$U = u/H$

u = Horizontal displacement

v = Vertical displacement

α_1 = Variation coefficient of c_1^2 due to depth from the earth surface.

α_2 = Variation coefficient of c_2^2 due to depth from the earth surface.

β = Angular displacement

$\eta = y/H$

λ = Lamé's elastic constant;

μ = Lamé's elastic constant

ν = Poisson's ratio

$\xi = x/a$

ρ = Density of the earth

ψ = Seismic earth pressure coefficient